

## Electronic Supporting Information

### Mechanoresponsive luminescence triggered by a supercooled transition of a copper(I) complex

Jérémy Delafoulhouze,<sup>a</sup> Marie Cordier,<sup>b</sup> Jean-Yves Mevellec,<sup>a</sup> Florian Massuyeau,<sup>a</sup> Olivier Hernandez,<sup>a</sup> Camille Latouche<sup>a,c</sup> and Sandrine Perruchas<sup>a\*</sup>

<sup>a</sup> Nantes Université, CNRS, Institut des Matériaux de Nantes Jean Rouxel, IMN, F-44000 Nantes, France.

Phone: (+33) (0)2 40 37 63 35. E-mail: sandrine.perruchas@cnrs-immn.fr

<sup>b</sup> Univ. Rennes, CNRS, ISCR (Institut des Sciences Chimiques de Rennes) - UMR 6226, F-35000 Rennes, France.

<sup>c</sup> Institut Universitaire de France (IUF), Paris F-75005, France.

#### Synthesis.

Copper(I) iodide, tetrabutylphosphonium iodide and the solvent were purchased from Aldrich and used as received.

**(PBU<sub>4</sub>)<sub>2</sub>[Cu<sub>2</sub>L<sub>4</sub>] (1As).** CuI (132 mg, 0.7 mmol) and PBU<sub>4</sub>I (267 mg, 0.7 mmol) were dissolved in 20 mL of acetonitrile. After complete dissolution, the solvent is evaporated leading to a viscous product forming rapidly a white powder with yield of 95 % (M = 1154 g.mol<sup>-1</sup>).

Anal. Calcd (% wt.) for **1As** for C<sub>32</sub>H<sub>72</sub>Cu<sub>2</sub>L<sub>4</sub>P<sub>2</sub>: C, 33.32; H, 6.29. Found: C, 33.14, H, 5.98.

Anal. Calcd (% wt.) for **1RE** for C<sub>32</sub>H<sub>72</sub>Cu<sub>2</sub>L<sub>4</sub>P<sub>2</sub>: C, 33.32; H, 6.29. Found: C, 33.03; H, 6.01.

#### Characterizations.

Elemental analyses (C, H, N) were performed by the Service de microanalyses de l'ICSN - CNRS Gif-sur-Yvette.

The TG (Thermogravimetric Analysis) analyses were performed with a NETZCH STA449 F3 equipment. The DSC (Differential Scanning Calorimetry) measurements were performed with a NETZSCH DSC 200 F3 equipment at 1 °C/min.

Luminescence spectra were recorded with a Fluorolog 3 spectrofluorimeter (Horiba Jobin Yvon). Low temperature measurements were realized in an OptistatDN-V Oxford cryostat. The absolute photoluminescence quantum yields (PLQY) were measured by using the Jobin Yvon integrating sphere. Emission lifetimes ( $\tau$ ) were recorded with a time-resolved photoluminescence setup consisting of a frequency-tripled regenerative amplified femtosecond Ti:sapphire laser system from Spectra Physics to obtain  $\lambda_{\text{ex}} = 267$  and 400 nm and a C7700 streak camera from Hamamatsu coupled to an SP2300 imaging Acton spectrograph for the luminescence detection. Data were analyzed by exponential curve fitting using *Origin* software.

Powder X-ray diffraction (PXRD) diagrams were recorded on a Bruker D8 Advance instrument in the Bragg-Brentano geometry, equipped with a front germanium monochromator, a copper anode (CuK-L3 radiation  $\lambda = 1.540598 \text{ \AA}$ ) and a LynxEye PSD detector. The calculated patterns were obtained from the single crystal data (SCXRD) using the *Mercury* software.

Single crystal X-Ray diffraction (SCXRD) analyses were performed on a crystal of **1** (colorless prism, dimensions = 0.450 x 0.330 x 0.250 mm) mounted on the goniometer head of a D8 Venture (Bruker-AXS) diffractometer equipped with a CMOS-PHOTON70 detector, using Mo- $K\alpha$  radiation ( $\lambda = 0.71073 \text{ \AA}$ , multilayer monochromator) at  $T = 297(2) \text{ K}$ . Crystal structure was solved by dual-space algorithm using *SHELXT* program,<sup>1</sup> and then refined with full-matrix least-squares methods based on  $F^2$  (*SHELXL*).<sup>2</sup> All non-Hydrogen atoms were refined with anisotropic atomic displacement parameters. H atoms were finally included in their calculated positions and treated as riding on their parent atom with constrained thermal parameters. The  $(\text{PBU}_4)^+$  cations present structural disorder with two positions for each, having 75/25 and 50/50 occupancy ratio. Details of the crystal data and structure refinements are summarized in Table S1.

Raman spectra from 73 to 1500  $\text{cm}^{-1}$  and from 2500 to 3500  $\text{cm}^{-1}$  were measured with a Raman T64000 Jobin Yvon triple spectrometer. All spectra were recorded using an excitation wavelength of 633 nm emitted by a Helium Neon laser. The Rayleigh line was eliminated with a premonochromator.

### Computational details.

Density Functional Theory (DFT) calculations were conducted using the Gaussian16 package<sup>3</sup> based on previous computations on  $(\text{PPh}_4)_2[\text{Cu}_2\text{I}_4]$ .<sup>4</sup> The PBE0 functional, in conjunction with the triple  $\zeta$  basis set DEF2TZVP for Cu and I atoms,<sup>5,6</sup> was employed to examine the  $[\text{Cu}_2\text{I}_4]^{2-}$  moiety within the ideal  $D_{2h}$  symmetry point group. Inner electrons (relativistic effects) were not explicitly treated, as they are accounted for in the pseudo-potentials. Spin-orbit coupling was not considered in this study. The vibrational analysis utilized the anharmonic GVPT2 model, as described in previous publications.<sup>7</sup> Within this model, it becomes feasible to simulate the Raman signature, including energies and intensities, while considering various anharmonic effects such as overtones, combination bands, Fermi, and Darling-Dennisson resonances. Given the small size of the structure under investigation, our analysis extended to computing second overtones (MaxQuanta=3). In this context, we identified a strong band at 105  $\text{cm}^{-1}$  corresponding to Cu-I stretching which must correspond to the experimental 120  $\text{cm}^{-1}$  band. Two vibrational overtones were also calculated at 138 and 147  $\text{cm}^{-1}$  (corresponding fundamentals peaking at 69 ( $b_{2g}$ , Cu-I twisting) and 73 ( $b_{3u}$ , Cu-I wagging)  $\text{cm}^{-1}$ , respectively). These vibrational overtones can correspond to the experimental 146  $\text{cm}^{-1}$  band.

## Additional Data.

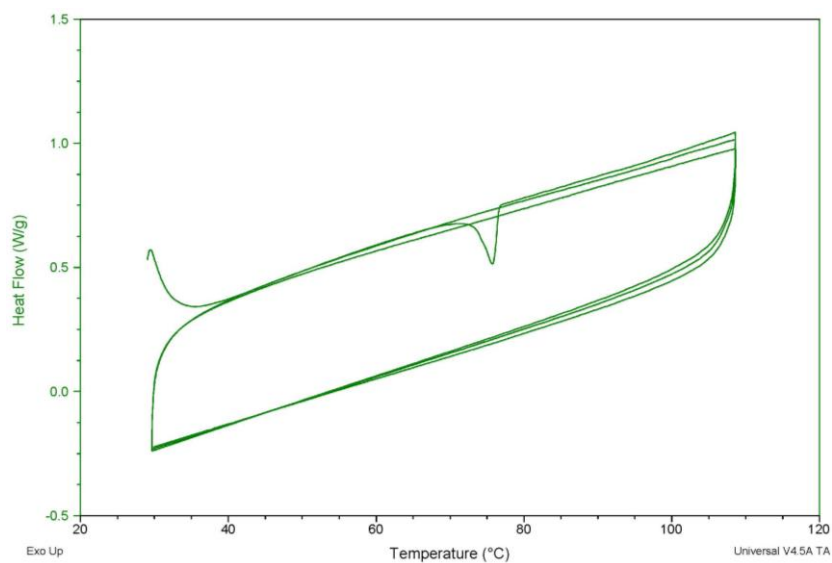


Figure S1. DSC (differential scanning calorimetry) curves of **1** at 1 °C/min.

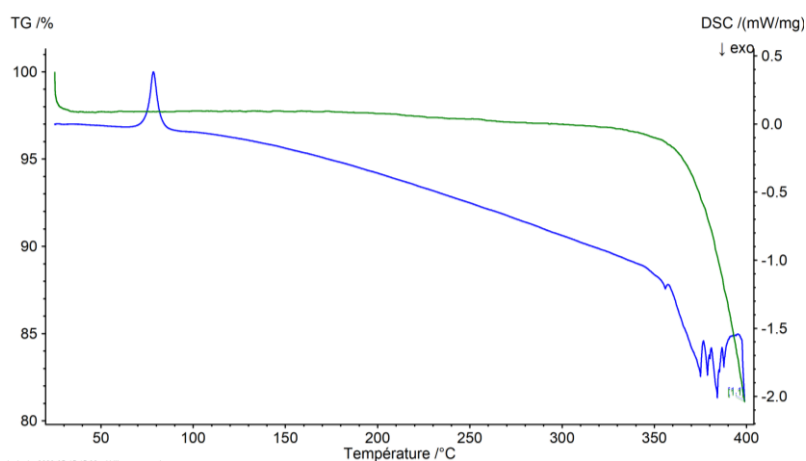


Figure S2. ATG-DTA curves of **1**.

Table S1. SCXRD and structure refinement data of  $(\text{Bu}_4\text{P})_2[\text{Cu}_2\text{I}_4]$  (**1**) at 293 K.

	<b><math>(\text{Bu}_4\text{P})_2[\text{Cu}_2\text{I}_4]</math></b>
CCDC n°	2314646
Chemical formula	$\text{C}_{32} \text{H}_{72} \text{P}_2 \text{Cu}_2 \text{I}_4$
fw	1153.51
Crystal system	Triclinic
Space group	$P - 1$
a, Å	12.4248(14)
b, Å	12.9746(16)
c, Å	16.828(2)

$\alpha$ , deg	86.253(5)
$\beta$ , deg	75.221(4)
$\gamma$ , deg	64.491(4)
$V$ , Å <sup>3</sup>	2364.3(5)
$Z$	2
$\rho_{\text{calc}}$ , g/cm <sup>3</sup>	1.620
$\mu$ , mm <sup>-1</sup>	3.596
Reflections collected	31523
Independent reflections	8951
$R_{\text{int}}$	0.0457
Reflections $I > 2\sigma(I)$	6254
Parameters	489
GOF on $F^2$	1.035
$R_1^a/wR_2^b$ ( $I > 2\sigma(I)$ )	0.0561/0.1429
$R_1^a/wR_2^b$ (all)	0.0807/0.1673

<sup>a</sup>  $R_1 = [\sum \text{abs}(\text{abs}(F_o) - \text{abs}(F_c))]/[\sum \text{abs}(F_o)]$ . <sup>b</sup>  $wR_2 = [\sum(w(F_o^2 - F_c^2)^2)/\sum(w(F_o^2)^2)]^{0.5}$ .

**Table S2.** Selected intramolecular bonds lengths and angles of (Bu<sub>4</sub>P)<sub>2</sub>[Cu<sub>2</sub>I<sub>4</sub>] (**1**) from SCXRD at 293 K.

	<b>1</b> CRYST
<b>Cu<sup>...</sup>Cu</b>	2.6576(14)
<b>Cu-I<math>\mu</math><sub>2</sub></b>	2.5450(12) 2.5805(12) 2.5855(12) 2.5924(13)
<b>Cu-I<math>\mu</math><sub>1</sub></b>	2.4936(11) 2.4907(12)
<b>I<math>\mu</math><sub>1</sub>-Cu-I<math>\mu</math><sub>2</sub></b>	125.02(4) 118.34(4) 122.03(5) 122.85(5)
<b>I<math>\mu</math><sub>2</sub>-Cu-I<math>\mu</math><sub>2</sub></b>	116.62(4) 115.12(4)
<b>I-Cu-I-Cu</b>	165.52(7) 164.75(7) 165.68(7) 164.59(7)

**Table S3.** Photophysical data of **1**.

	$\lambda_{\max}$ (nm)	PLQY	$\tau$ ( $\mu\text{s}$ )	$k_r$ ( $\mu\text{s}^{-1}$ )	$k_{nr}$ ( $\mu\text{s}^{-1}$ )
<b>1<sub>AS</sub></b>	520	0.90	4.6	0.20	0.02
<b>1<sub>sc</sub></b>	650	0.04	0.47	0.09	2.04
<b>1<sub>RE</sub></b>	520	0.87	3.0	0.29	0.04

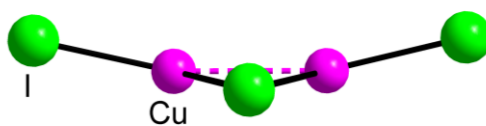


**Figure S3.** Molecular structure of  $[\text{Cu}_2\text{I}_4]^{2-}$  anion showing its folded geometry with  $\text{I}\mu_1\text{-Cu-I}\mu_2\text{-Cu}$  mean torsional angles of  $165.14(7)^\circ$  at 293 K.

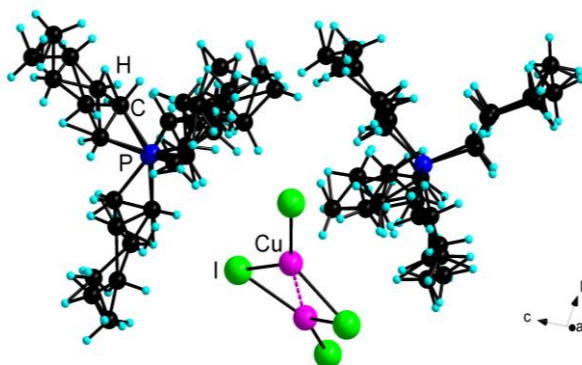


**Figure S4.** Molecular structure of  $(\text{Bu}_4\text{P})_2[\text{Cu}_2\text{I}_4]$  (**1**) showing the structural disorder of the two  $(\text{Bu}_4\text{P})^+$  cations at 293 K.

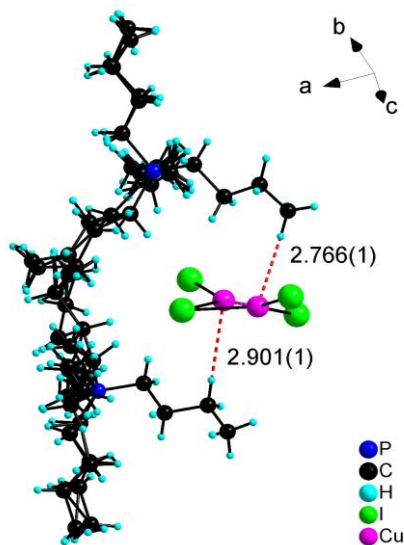


**Figure S5.** Intermolecular Cu...H contacts in **1** structure at 293 K.

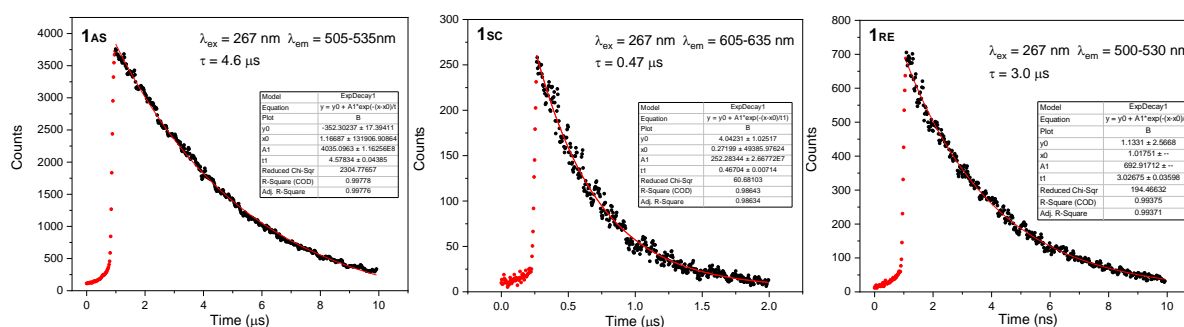


**Figure S6.** Fitted emission decay curves at 293 K. The red dots are not considered for the fits.

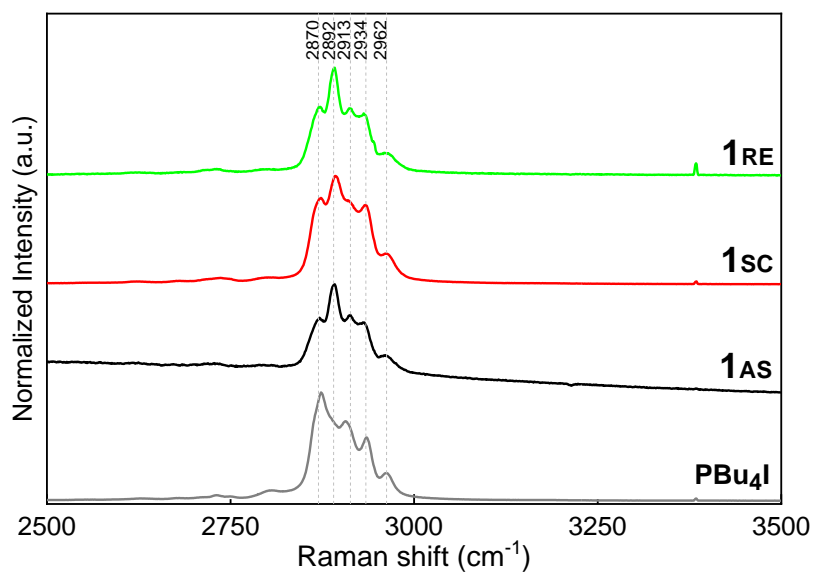


**Figure S7.** Raman spectra of **1**, as synthesized (**1AS**), in the supercooled state (**1sc**) and in the mechanically recrystallized state (**1RE**), from 2500 to 3500  $\text{cm}^{-1}$  at 293 K. The vibrations are from the butyl chains of the  $(\text{Bu}_4\text{P})^+$  cation.

## References SI

---

- (1) Sheldrick, G. M.; *Acta Cryst.* 2015, **A71**, 3-8.
- (2) Sheldrick G. M.; *Acta Cryst.* 2015, **C71**, 3-8.
- (3) Gaussian 16, Revision A.03, M. J. Frisch, G. W. Trucks, H. B. Schlegel, G. E. Scuseria, M. A. Robb, J. R. Cheeseman, G. Scalmani, V. Barone, G. A. Petersson, H. Nakatsuji, X. Li, M. Caricato, A. V. Marenich, J. Bloino, B. G. Janesko, R. Gomperts, B. Mennucci, H. P. Hratchian, J. V. Ortiz, A. F. Izmaylov, J. L. Sonnenberg, D. Williams-Young, F. Ding, F. Lipparini, F. Egidi, J. Goings, B. Peng, A. Petrone, T. Henderson, D. Ranasinghe, V. G. Zakrzewski, J. Gao, N. Rega, G. Zheng, W. Liang, M. Hada, M. Ehara, K. Toyota, R. Fukuda, J. Hasegawa, M. Ishida, T. Nakajima, Y. Honda, O. Kitao, H. Nakai, T. Vreven, K. Throssell, J. A. Montgomery, Jr., J. E. Peralta, F. Ogliaro, M. J. Bearpark, J. J. Heyd, E. N. Brothers, K. N. Kudin, V. N. Staroverov, T. A. Keith, R. Kobayashi, J. Normand, K. Raghavachari, A. P. Rendell, J. C. Burant, S. S. Iyengar, J. Tomasi, M. Cossi, J. M. Millam, M. Klene, C. Adamo, R. Cammi, J. W. Ochterski, R. L. Martin, K. Morokuma, O. Farkas, J. B. Foresman, and D. J. Fox, Gaussian, Inc., Wallingford CT, 2016. Gaussian, Inc.
- (4) Thefioux, Y.; Cordier, M.; Massuyeau, F.; Latouche, C.; Martineau-Corcus, C.; Perruchas, S. *Inorg. Chem.* 2020, **59** (8), 5768–5780.
- (5) (a) Perdew, J. P.; Ernzerhof, M.; Burke, K. M. Rationale for Mixing Exact Exchange with Density Functional Approximations. *J. Chem. Phys.* 1996, **105**, 9982-9985. (b) Perdew, J. P.; Burke, K.; Ernzerhof, M.; Generalized Gradient Approximation Made Simple. *Phys. Rev. Lett.* 1996, **77**, 3865-3868. (c) Perdew, J. P.; Burke, K.; Ernzerhof, M. Erratum: Generalized Gradient Approximation Made Simple. *Phys. Rev. Lett.* 1997, **78**, 1396-1396.
- (6) (a) Dunning Jr., T. H.; Hay, P. J. *Methods of Electronic Structure Theory*, H. F. Schaeffer ed., Plenum Press, New York, 1977. (b) Hay, P. J.; Wadt, W. R. Ab Initio Effective Core Potentials for Molecular Calculations. Potentials for the Transition Metal atoms Sc to Hg. *J. Chem. Phys.* 1985, **82**, 270-283. (c) Hay, P. J.; Wadt, W. R. Ab Initio Effective Core Potentials for Molecular Calculations. Potentials for the Main Group Elements Na to Bi. *J. Chem. Phys.* 1985, **82**, 284-298. (d) Hay, P. J.; Wadt, W. R. Ab Initio Effective Core Potentials for Molecular Calculations. Potentials for K to Au Including the Outermost Core Orbitals. *J. Chem. Phys.* 1985, **82**, 299-310.
- (7) (a) Barone, V. *J. Chem. Phys.* 2005, **122**, 014108; (b) Barone, V.; Biczysko, M.; Bloino, J. *Phys. Chem. Chem. Phys.* 2014, **16**, 1759-1787; (c) Bloino, J. *J. Phys. Chem. A* 2015, **119**, 5269–5287.